Molecular Crystals and Liquid Crystals

Publication details, including instructions for authors and subscription information:
http://www.tandfonline.com/loi/gmcl20

Sudden Isotropic-Nematic Phase Transition Within a Plan-Parallel Cell

Marjan Krasna [a], Robert Repnik [a], Zlatko Bradac [a] & Samo Kralj [a]

[a] Department of Physics, Faculty of Education, Koroska, Maribor, Slovenia

Version of record first published: 31 Aug 2006

To cite this article: Marjan Krasna, Robert Repnik, Zlatko Bradac & Samo Kralj (2006): Sudden Isotropic-Nematic Phase Transition Within a Plan-Parallel Cell, Molecular Crystals and Liquid Crystals, 449:1, 127-135

To link to this article: http://dx.doi.org/10.1080/15421400600582606

Mol. Cryst. Liq. Cryst., Vol. 449, pp. 127–135, 2006

ISSN: 1542-1406 print/1563-5287 online
DOI: 10.1080/15421400600582606

Taylor & Francis
Taylor & Francis Group

Sudden Isotropic-Nematic Phase Transition Within a Plan-Parallel Cell

Marjan Krasna
Robert Repnik
Zlatko Bradac
Samo Kralj
Department of Physics, Faculty of Education, Koroska,
Maribor, Slovenia

We study the nematic structure of a liquid crystal confined within a plan-parallel cell following the temperature driven isotropic-nematic phase transition quench. The Lebwohl-Lasher lattice model is used. The kinetics of the system is followed via Brownian molecular dynamics, enabling us to reach macroscopic time scales. In the simulation we assume that at one confining plate the nematic pattern becomes imprinted and frozen in after the phase transition. We study the main features of resulting nematic equilibrium structures.

Keywords: nematic liquid crystals; phase transition; surface memory effects; surfaces

1. INTRODUCTION

Liquid crystal (LC) structures strongly depend on conditions at confining boundaries [1]. Particularly because of their use in various electro-optic applications there is a constant interest for studies on the influence of different mechanisms on boundary conditions. There are many cases where surface memory effects (SME) play important role [2]. For example, the onset of chevron structures in smectic liquid crystals confined within plan-parallel cells is attributed to SME [3,4]. Despite the importance of SME on LC structures relatively few studies focused on their understanding.

In this paper we study numerically the influence of SME on nematic structures within a plan-parallel cell. We use Lebwohl-Lasher lattice

Address correspondence to Marjan Krasna, Department of Physics, Faculty of Education, Koroska 160, 2000 Maribor, Slovenia. E-mail: marjan.krasna@uni-mb.si

model and Brownian molecular dynamics. The plan of the paper is as follows. In Sec. 2 we present the model used. The results are shown in Sec. 3. In the last section we summarize our results.

2. MODEL

2.1. Interaction Potential and Dynamics

In our semi-microscopic description we use the Lebwohl-Lasher model [5]. The interaction g_{ij} between a pair of rod-like LC *molecules* at $\vec{r}_i$ and $\vec{r}_j = \vec{r}_i + \Delta\vec{r}$, oriented along unit vectors $\vec{e}_i$ and $\vec{e}_j$, is expressed as [5,6]

$$g_{ij} = -\frac{J}{\Delta r^6}\left(\vec{e}_i \cdot \vec{e}_j\right)^2, \tag{1}$$

where J is a positive interaction constant.

The interaction energy of the whole sample is calculated as the sum of all pair interactions in the sample. Note that the original Lebwohl-Lasher model applies to the simple cubic lattice, taking into account only the nearest-neighbour interactions. In the simulation we restrict the interaction volume to a sphere of radius $2a_0$, where a_0 stands for the characteristic length of the cubic lattice. The number of *molecules* in simulation ranges from 10^4 to 10^6.

A local orientation of the i-th *molecule* in the laboratory coordinate system (x,y,z) is parametrized as $\vec{e}_i = (\sin\theta\cos\phi, \sin\theta\sin\phi, \cos\theta)$. The angles $\theta = \theta(\vec{r}_i, t)$ and $\phi = \phi(\vec{r}_i, t)$ are dynamic variables of the model. The rotational dynamics of the system is followed using the Brownian molecular dynamics [6,7]. At each time interval Δt (one sweep) the molecular orientation at the i-th site in the local cartesian frame (x′, y′,z′) is updated obeying the equations [6]

$$\begin{aligned} \vartheta_i^{(x')} &= -\frac{D\Delta t}{k_B T}\sum_{j\neq i}\frac{\partial g_{ij}}{\partial \vartheta_i^{(x')}} + \vartheta_{r,i}^{(x')}, \\ \vartheta_i^{(x')} &= -\frac{D\Delta t}{k_B T}\sum_{j\neq i}\frac{\partial g_{ij}}{\partial \vartheta_i^{(y')}} + \vartheta_{r,i}^{(y')}. \end{aligned} \tag{2}$$

Here k_B is the Boltzman constant, T is the temperature, and D the rotational diffusion constant. The z′-axis of the local frame is directed along the long molecular axis of the i-th molecule. The angles $\vartheta_i^{(x')}$ and $\vartheta_i^{(y')}$ correspond to small rotation about x′ and y′ axes. The gradient of the potential for these two rotations is calculated numerically. The quantities $\vartheta_{r,i}^{(x')}$ and $\vartheta_{r,i}^{(y')}$ are stochastic variables obeying the Gaussian distribution. The probabilities are centred at $\vartheta_{r,i}^{(x')} = \vartheta_{r,i}^{(y')} = 0$ and the widths $\Delta\vartheta_{r,i}^{(x')} = \Delta\vartheta_{r,i}^{(y')}$ of the distribution are proportional to $\sqrt{T}$.

A corresponding model in the continuum limit is roughly the Landau-de Gennes (LdG) approach [8] in terms of the tensor order parameter Q in the approximation of equal Frank elastic constants [9,10]. The link between the LdG meso-scopic and our semi-microscopic ordering is roughly given by

$$Q(\vec{r}_i) \approx \langle \vec{e}_i \otimes \vec{e}_i - I/3 \rangle, \tag{3}$$

where $<\ldots>$ stands for the time averaging over a relatively short time scale and over the neighbouring sites. In the case of uniaxial meso-scopic ordering one commonly expresses the order parameter as

$$Q = S(\vec{n} \otimes \vec{n} - I/3). \tag{4}$$

Here S stands for the uniaxial order parameter and $\vec{n}$ is the nematic director field. A convenient measure of biaxial ordering is given by the quantity [11,12]

$$\beta = 1 - 6\frac{(TrQ^3)^2}{Tr(Q^2)^3}. \tag{5}$$

This parameter ranges in the interval between $\beta = 0$ and $\beta = 1$. These limiting values reflect an uniaxial state and a state with maximal biaxiality, respectively.

In the simulation we calculate at each point the tensor order parameter using Eq. (3). We carry out the time averaging over 15 sweeps and consider averaging over 9^3 neighbouring sites.

2.2. Geometry

The geometry of the problem is depicted in Figure 1. The LC molecules are enclosed in a plan-parallel cell of thickness L. At the left plate ($z = 0$) we enforce isotropic tangential anchoring and at the right one ($z = L$) homogeneous tangential anchoring along the x-coordinate. At the lateral boundaries we use the periodic boundary condition. In the picture we also schematically show two qualitatively different scenarios how eventual local boundary conditions at opposing plates could be resolved in case of competing surface imposed ordering tendencies. The average orientational ordering of molecules (i.e., the mesoscopic perspective) in the cell for the two scenarios is depicted with 3D boxes. In (a) the contradicting surface tendencies are resolved via a rotation of LC molecules, and in (b) by changing their effective shape. Only the case (a) can be described in the uniaxial representation (i.e., by Eq. (4)). However, this scenario can be locally

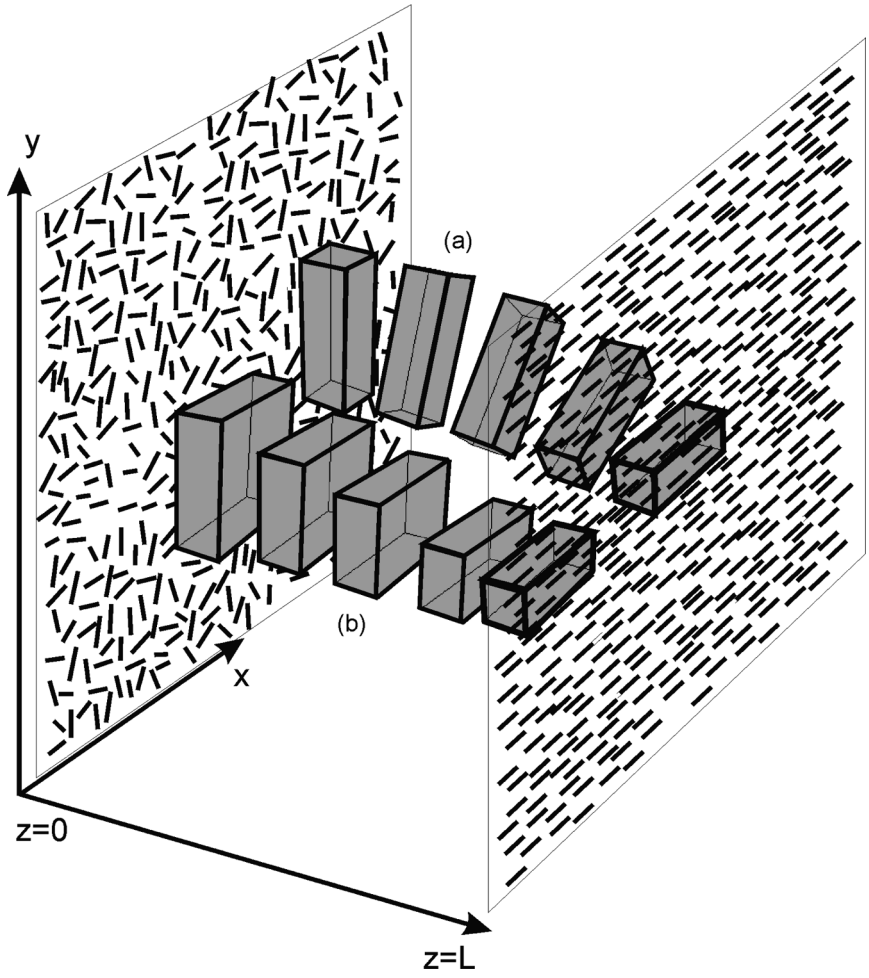

FIGURE 1 Schematic presentation of the geometry used in the simulation. The cell plates are set at z = 0 and z = L. At z = 0 we enforce strong isotropic tangential anchoring after time t_f. At z = L we set strong tangential anchoring along the z-axis. Two qualitatively different scenario are also plotted in which contradicting tendencies imposed by the confining plates are resolved.

realized only above a large enough (in comparison to the biaxial correlation length) frozen-in domain at the left side of Figure 1, the average orientation of which differs from the one enforced by the plate on the right.

3. RESULTS

In the simulation we quench the system from the isotropic phase deep into the nematic phase. Soon after the quench the domain pattern is formed due to the symmetry breaking and causality. Namely, in the high temperature phase the system displays a continuous symmetry. After the quench in causally disconnected parts of the system a random value of symmetry breaking order parameter value is chosen depending on a local preference mediated by a fluctuation. Consequently a domain structure appears characterized by a single domain length ξ_d. The subsequent domain growth gradually enters the dynamic scaling regime, where the power law $\xi_d \propto t^{\gamma}$ is obeyed. In the bulk one expects $\gamma \approx 0.5$ [6]. The order parameter evolution across a domain wall obeys geodesic rule, i.e., it follows the shortest possible path in the order parameter space.

A typical time evolution of ξ_d and of the average uniaxial order parameter $\langle S \rangle$ of the system are plotted in Figure 2. In this approach we estimate ξ_d of an average domain using the geometric approach. We calculate an average volume V_d in which there are relatively small changes of the orientational ordering. As the criteria of being in a domain we set $|\vec{e}_i \cdot \vec{e}_j| > 0.8 \approx 2\cos(\Delta\theta_r)$, where the indices (i,j) locate

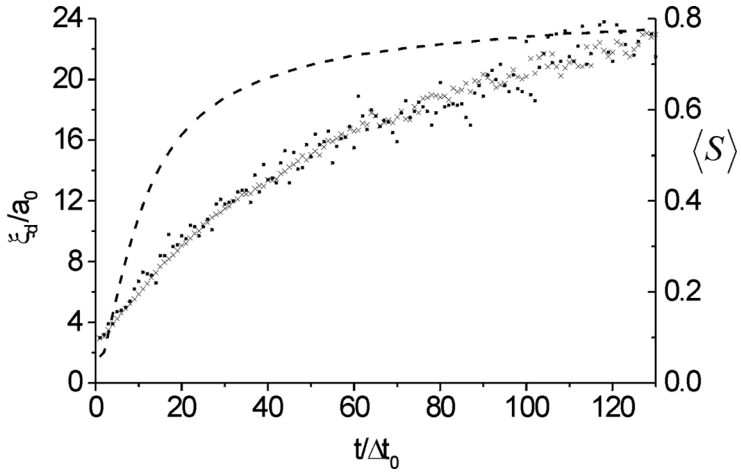

FIGURE 2 Time evolution of $\langle S \rangle$ (dashed line) and ξ_d in bulk. The dotted line shows $\xi_d(t)$ dependence calculated using the geometric approach. The line marked with (x) is calculated on energy grounds, as described in Ref. [6]. Δt_0 indicates the time within averaging is taken (i.e., 15 sweeps were taken inside Δt_0).

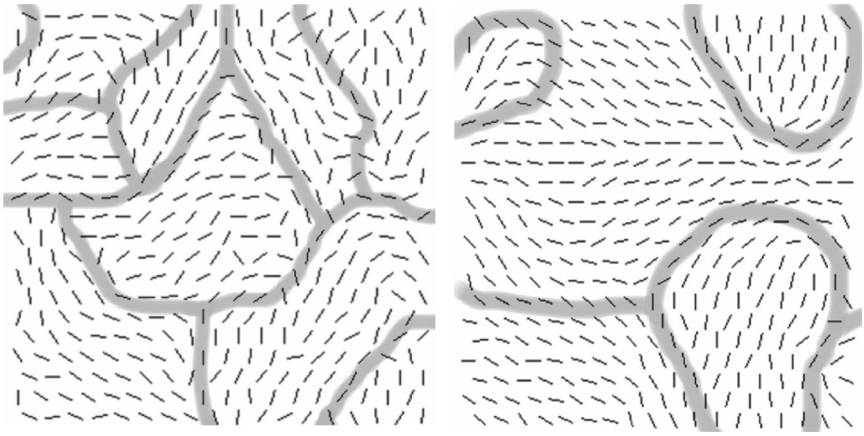

FIGURE 3 Frozen in pattern in the (x,y) plane at z = 0 for (a) n = 4, and (b) n = 2. The thick lines indicate domain boundaries.

neighbouring molecules. The domain size is then estimated as $\xi_d \approx (6V_d/\pi)^{1/3}$. The average $\langle S \rangle$ was obtained by diagonalizing the tensor order parameter (Eq. (3)) at each site and taking the average over all the sites. After a time t_f, when the degree of ordering is high enough, we set $\theta(x,y,z=0) = \pi/2$ and froze in the established domain pattern at $z = 0$. We determine t_f from the condition $\langle S \rangle \approx S_b/n$, where S_b stands for the equilibrium value of $\langle S \rangle$ and $n \approx 2$. In Figure 3 we show typical frozen domain patterns at z = 0 (the left plate in Fig. 1) for n = 2, and n = 4. A typical cross-sections in the (x,z) plane at different times t is shown in Figure 4. With time t the domain structure of the system on average decays, while the surface layer at $z = 0$ tends to conserve the domain structure. After a long enough time (i.e., 10000 sweeps for $N = 10^4$) the equilibrium pattern is formed characterized by a biaxial layer of thickness ξ_b. The thickness of the surface layer is weakly dependent on L. Our simulations suggest $\xi_b \approx 10a_0$. Above it essentially uniform structure exists aligned on average along the x-axis. The value of ξ_b was determined from the z-dependence of the biaxial parameter $\langle \beta \rangle_\perp$, where $\langle \ldots \rangle_\perp$ refers to the averaging in a (x,y) plane. Plots of $\langle \beta \rangle_\perp$ as a function of z for different values of L are shown in Figure 5.

4. CONCLUSIONS

We study the influence of surface memory effects on equilibrium nematic structures within a plan-parallel cell deep in the nematic

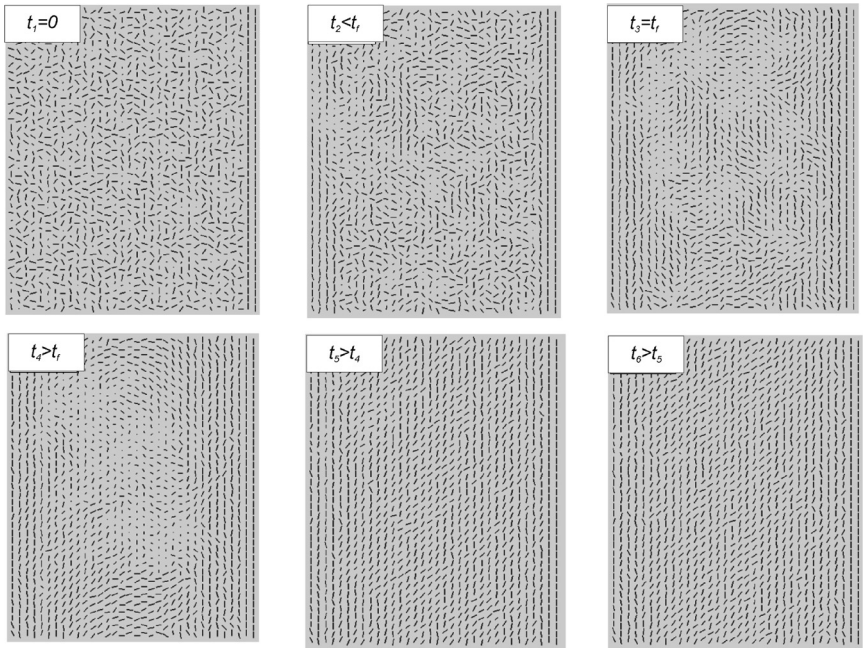

FIGURE 4 Cross sections in a (x,z) plane are shown at different times.

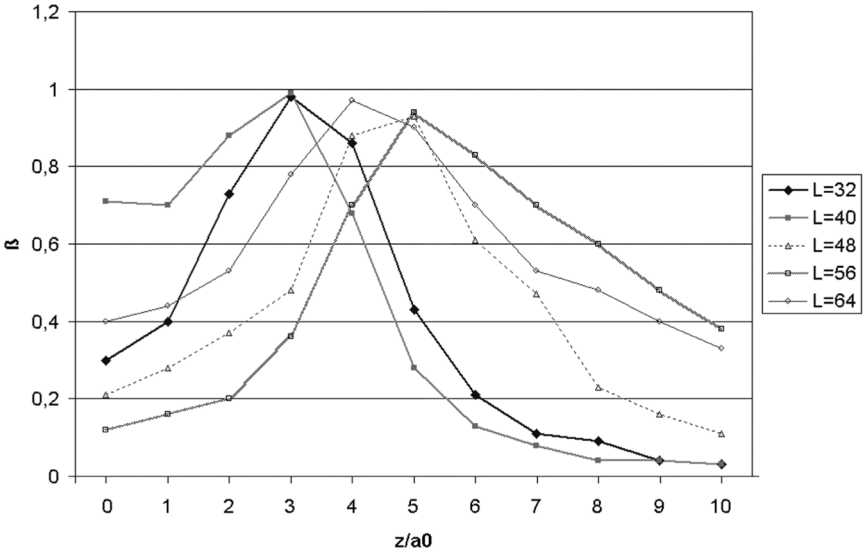

FIGURE 5 Plot of $\langle\beta\rangle_{\perp}$ as a function of z for different values of L.

phase. We use Lebwohl-Lasher interaction potential and follow the kinetics via Brownian molecular dynamics. In the simulation we quench the system from the isotropic phase deep into the nematic phase. Consequently a domain pattern is formed. After some time, where the average degree of ordering within the cell is strong enough, we freeze in the orientational ordering of LC molecules at one plate. This frozen pattern serves afterwards as a boundary condition for the nematic ordering within the cell. We show that a biaxial layer is formed, whose length weakly depends on the cell thickness. Its detailed structure depends on the value $\langle S \rangle$ and the domain length ξ_d at the freez-in time t_f. Therefore the final structure memorizes the established state at t_f. In the simulation we have assumed that a critical value of $\langle S \rangle$ determines t_f. In cases studied in this contribution we have limited to sudden quenches. Quenches have been realised fast in comparison to the order parameter relaxation time. In such cases the frozen-in domains are comparable to the biaxial correlation length. Consequently a relatively strong biaxiality appears that is essentially homogeneously distributed in a (x,y) plane just above the frozen layer. This situation can change if $\xi_d(t_f)$ apparently exceeds the biaxial correlation length. Such scenario could be realized in relatively slow quenches which is the focus of our future study.

REFERENCES

[1] Jerome, B. (1991). Surface effects and anchoring in liquid crystals. *Rep. Prog. Phys.*, *54*, 391.
[2] Tao, R., Sheng, P., & Lin, Z. F. (1993). Nematic-isotropic phase transition: An extended mean field theory. *Phys. Rev. Lett.*, *70*, 1271.
[3] Rieker, T. P., Clark, N. A., Smith, G. S., Parmar, D. S., Sirota, E. B., & Safina, C. R. (1987). "Chevron" local layer structure in surface-stabilized ferroelectric smectic-C cells. *Phys. Rev. Lett.*, *59*, 2658.
[4] Kralj, S. & Sluckin, T. J. (1994). Landau–de Gennes theory of the chevron structure in a smectic-A liquid crystal. *Phys. Rev. E.*, *50*, 2940.
[5] Lebwohl, P. A. & Lasher, G. (1972). Nematic-liquid-crystal order—A Monte Carlo calculation. *Phys. Rev. A., 6*, 426.
[6] Bradač, Z., Kralj, S., & Žumer, S. (2002). Molecular dynamics study of the isotropic-nematic quench. *Phys. Rev. E., 65*, 021705.
[7] Ermak, D. L. (1975). A computer simulation of charged particles in solution. I. Technique and equilibrium properties. *J. Chem. Phys.*, *62*, 4189.
[8] de Gennes, P. G. & Prost, J. (1993). *The Physics of Liquid Crystals*, Oxford University Press: Oxford.
[9] Barbero, G. & Evangelista, L. R. (2001). *Elementary Course on the Continuum Theory for Nematic Liquid Crystals*, World Scientific: Singapore.
[10] Bradač, Z., Kralj, S., & Žumer, S. (1998). Molecular dynamics study of nematic structures confined to a cylindrical cavity. *Phys. Rev. E., 58*, 7447.

[11] Kaiser, P., Wiese, W., & Hess, S. (1992). Stability and instability of a uniaxial alignment against biaxial distortions in the isotropic and nematic phases of liquid crystals. *J. Non-Equilib. Thermodyn.*, *17*, 153.
[12] Kralj, S., Virga, E. G., & Žumer, S. (1999). Biaxial torus around nematic point defects. *Phys. Rev. E., 60*, 1858.